Microwave Spectrum, Dipole Moment, and Internal Dynamics of the Methyl Fluoride−Carbonyl Sulfide Weakly Bound Complex

Michal M. Serafin and Sean A. Peebles*

Department of Chemistry, Eastern Illinois University, 600 Lincoln Avenue, Charleston, Illinois 61920

Received: October 19, 2007; In Final Form: November 13, 2007

Rotational spectra for the normal and four isotopically substituted species of the 1:1 complex between methyl fluoride (H_3CF) and carbonyl sulfide (OCS) have been measured using Fourier-transform microwave spectroscopy in the 5−16 GHz frequency region. The observed spectra fit well to a semirigid Watson Hamiltonian, and an analysis of the rotational constants has allowed a structure to be determined for this complex. The dipole moment vectors of the H_3CF and OCS monomers are aligned approximately antiparallel with a C···C separation of 3.75(3) Å and with an *ab* plane of symmetry. The values of the P_{cc} planar moments were found to be considerably different from the expected rigid values for all isotopologues. An estimate of ∼14.5(50) cm^{-1} for the internal rotation barrier of the CH_3 group with respect to the framework of the complex has been made using the P_{cc} values for the H_3CF−OCS and D_3CF−OCS isotopic species. Two structures, very close in energy and approximately related by a 60° rotation about the C_3 axis of the methyl fluoride, were identified by ab initio calculations at the MP2/6-311++G(2d,2p) level and provide reasonable agreement with the experimental rotational constants and dipole moment components.

Introduction

Fluorinated methanes are ideal prototype molecules for systematically studying the effects of the changing acidity of the CH proton on the intermolecular structural parameters of complexes that exhibit C−H···X contacts (where X = O, N, or F). Data on complexes of trifluoromethane (HCF_3, TFM)[1−6] and difluoromethane (H_2CF_2, DFM)[7−11] form a reasonably large body of information in the literature, while studies on the monosubstituted methyl fluoride are relatively scarce.[3] The methyl fluoride complex with trifluoromethane, H_3CF−TFM,[3] provides a particularly interesting example as a result of multiple C−H···F links. Spectral evidence for the internal rotation of both subunits within the complex was observed, although the barrier of rotation for the CH_3 group (V_3 ∼ 0.36 kJ mol^{-1}, corresponding to a reduced barrier, *s*, of 2.5) was determined to be considerably lower than that of the CF_3 group (V_3 = 0.840 kJ mol^{-1}, *s* = 67.92),[3] so *E*-state transitions were observable only for the rotation of the HCF_3 subunit. The *E* state lines arising from the internal rotation of the CH_3 group were shifted far outside of the accessible spectral region.

For complexes of TFM, a wide range of V_3 barriers has been observed, from around ∼0.5 kJ mol^{-1} (leading to *A*−*E* splittings of only a few tens of kHz (such as was seen in the spectra of the oxirane[1] and thiirane[2] complexes)) to almost free rotation (such as in benzene−TFM[5] where excited torsional states were observed).

In our laboratory, binary complexes of TFM and DFM with the simple linear molecules OCS,[12,13] CO_2,[14] and HCCH[15] have been studied, and only in TFM−CO_2 have *A* and *E* states arising from internal rotation of the TFM so far been unambiguously assigned, although considerable congestion in the spectrum of the very near prolate HCCH−TFM suggests the existence of substantial nonrigidity.[15]

In an attempt to add to the body of data on methyl fluoride complexes, the current paper extends our own studies of fluorinated methanes complexed with simple linear molecules[12−15] with a report on a study of the methyl fluoride−carbonyl sulfide complex. In light of the quite low barrier predicted for rotation of the H_3CF subunit in the H_3CF−TFM complex,[3] it was anticipated that location of the *E* state lines in H_3CF−OCS might be challenging due to large (potentially several gigahertz) *A*−*E* splittings, and indeed, no assignment of these lines has yet been made.

Experimental Section

Rotational spectra were measured with a Balle−Flygare[16] type Fourier-transform microwave spectrometer operating in the 5−16 GHz frequency range. This spectrometer has been discussed previously,[17] and the design is based upon instrumentation developed at the University of Kiel in the early 1990s.[18] Gas samples consisted of approximately 1.5% of each gas component (OCS, Sigma-Aldrich; H_3CF, Matheson TriGas), diluted in first-run He/Ne carrier gas (17.5% He: 82.5% Ne, BOC Gases) to a total pressure of 2−2.5 bar. This gave rise to rotational transitions of optimum intensity that remained strong throughout several dilutions with He/Ne during the searching and measuring process. The gas mixture was expanded into the vacuum chamber by means of a General Valve Series 9 solenoid valve with a 0.8 mm orifice. Stark effect measurements were carried out by application of electric potentials of up to ±5 kV to a pair of 30 cm square steel mesh plates, placed within the vacuum chamber, straddling the molecular expansion, and located about 30 cm apart. Calibration of the electric field was achieved using the $J = 1 \leftarrow 0$ transition of OCS at 12162.979 MHz and assuming a dipole moment of μ = 0.71521(20) D.[19] Spectra for D_3CF−OCS, $H_3{}^{13}CF$−OCS, and H_3CF−$O^{13}CS$ were measured using isotopically enriched samples (D_3CF, 99%+ D, Isotec; $H_3{}^{13}CF$, 99% ^{13}C, Icon Isotopes; $O^{13}CS$, 99% ^{13}C,

* To whom correspondence should be addressed. E-mail: sapeebles@eiu.edu. Phone: (217) 581-2679. Fax: (217) 581-6613.

10.1021/jp710181z CCC: $40.75
Published on Web 01/25/2008

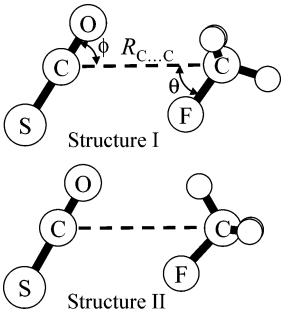

Figure 1. Structures I and II obtained from the MP2/6-311++G(2d,2p) ab initio optimizations. Structure I was only higher in energy than structure II by 0.5 cm^{-1} (BSSE- and zero-point-uncorrected). The three parameters ($R_{C\cdots C}$, θ, and ϕ) used in the structure fitting procedure are also defined.

Icon Isotopes), while the $H_3CF-OC^{34}S$ spectrum was measured in natural abundance (~4%).

Results

Ab Initio Calculations. Ab initio investigations to identify the lowest-energy structures for the $H_3CF-OCS$ complex were carried out at the MP2/6-311++G(2d,2p) level using Gaussian 03[20] running on a Linux workstation. These calculations allowed identification of the initial search region and also provided a crude estimate for the barrier of rotation. Ab initio calculations for similar complexes at similar levels of theory have been observed to provide reasonable estimates of the structure[12,14,15] but often do rather poorly in providing quantitative estimates of the internal rotation barrier. For example, overestimates of the barrier by 30−70% have been seen in previous studies of TFM complexed with oxirane[1] and thiirane,[2] even when corrections for basis set superposition error (BSSE) were included. Nevertheless, such calculations do serve as a useful guide to the expected order of magnitude of the barrier and hence the relative magnitude of the internal rotation splittings which may be expected in the rotational spectrum. The calculations used for initial location of the spectrum of $H_3CF-OCS$ were carried out initially with no BSSE and zero-point energy (ZPE) corrections, although a counterpoise-corrected optimization utilizing the COUNTERPOISE keyword in Gaussian 03 later revealed that the relative stability is very sensitive to these corrections (see below). Nonetheless, it was apparent that the two lowest-energy structures (I and II) shown in Figure 1 were very close in energy, with structure II found to be the most stable at all but the BSSE+ZPE-corrected level (Table 1). Less than 0.5 cm^{-1} separates I and II at the BSSE- and ZPE-uncorrected level; when the BSSE-corrected optimization is carried out, this difference increases to 16.3 cm^{-1}. Interestingly, when ZPE corrections are then applied to the BSSE-optimized structure, the order of stability switches, with structure I becoming the most stable by 7.5 cm^{-1}. Although these calculations are relatively crude, they do highlight the small energy difference between the two forms, and interconversion between them is likely even at the low temperatures of the supersonic beam. A single imaginary frequency (10*i* cm^{-1}) is found at the BSSE+ZPE-corrected level for structure I; this vibrational mode is a torsional motion of the CH_3F about its C_3 axis, which interconverts structures I and II.

At both the uncorrected and BSSE-corrected levels, the structural parameters of I and II do differ slightly (quite significantly so in the case of the intermolecular C···C distance, where the values differ by more than 0.1 Å); therefore, the two ab initio minima are not simply related by a 60° rotation about the C_3 axis. Of course, it is possible to adjust the intermolecular distance and relative tilt angles (see Figure 1) such that the same set of values are obtained for the three structural parameters regardless of whether the H atom that is located in the *ab* symmetry plane is pointing toward or away from the OCS molecule (this will be addressed in more detail in the Structure section). The differences in the two ab initio structures might be attributed to (i) a very flat potential energy surface leading to slight differences in the converged structures or (ii) the fact that the internal rotation axis may not coincide exactly with the C_3 axis of the MeF, and hence, the minimum and the transition-state structures may differ by more than a straightforward rotation about that axis. The ab initio structural parameters, rotational constants, and relative energies from the uncorrected and BSSE-corrected calculations are summarized in Table 1 for structures I and II. It should be noted that the difference in the rotational constants for the two structures is about the same as the usual degree of uncertainty in the ab initio rotational constants for a weakly bound complex of this nature (typically about 1−5%).

TABLE 1: Structural Parameters and Rotational Constants Obtained from the Ab Initio (MP2/6-311++G(2d,2p)) Optimizations on Structures I and II; See Figure 1 for a Definition of the Structural Parameters

parameter[a]	structure I	structure II
$R_{C\cdots C}$/Å	3.63 (3.75)	3.75 (3.86)
θ/degrees	53.5 (54.3)	48.4 (49.2)
ϕ/degrees	58.1 (58.1)	61.1 (60.4)
A/MHz	7267 (7156)	7121 (7117)
B/MHz	1690 (1591)	1661 (1566)
C/MHz	1383 (1312)	1358 (1294)
relative energy/cm^{-1}	0.5 (16.3, −7.5)[b]	0

[a] The structural parameters and rotational constants are given first for the BSSE-uncorrected calculation, with the values obtained from a BSSE-corrected optimization given in parentheses. [b] Three values are given for the relative energy of structure I; the first is BSSE- and ZPE-uncorrected, while the two energies in parentheses refer to BSSE-corrected and BSSE+ZPE-corrected values, respectively. The −7.5 cm^{-1} value implies that in the BSSE+ZPE-corrected case, structure I was actually determined to be more stable than II (see text for discussion).

Spectra and Estimated Barrier to Rotation. Spectral searches based on the ab initio optimizations discussed in the previous section enabled the *a*-type spectrum of a near prolate asymmetric top ($\kappa \sim -0.90$) to be readily assigned, giving precise values of the rotational constants *B* and *C*. These *a*-type transitions were very intense, having signal-to-noise ratios in excess of 80 in 100 gas pulses. However, location of the *b*-type spectrum proved more challenging. If the complex possesses an *ab* plane of symmetry (as expected from the ab initio results), then the planar moment P_{cc} of the complex should lie close to the value of P_{bb} for the methyl fluoride monomer ($P_{bb}(H_3CF) = 1.62656(1)$ u Å^2)[21] since only H atoms are situated out of the *ab* symmetry plane. Attempts to locate these transitions using any physically reasonable value of P_{cc}(complex) to estimate the value of the *A* rotational constant were not successful. The $1_{11} \leftarrow 0_{00}$ *b*-type transition was eventually located about 470 MHz away from this predicted frequency; the resulting rotational constants gave a nonphysical P_{cc} planar moment of −0.21938(15) u Å^2 for the normal isotopic species. Similar behavior was observed for all isotopologues, where the value of P_{cc} was considerably less than the expected rigid value; for all H_3CF species, it was consistently approximately −0.22 u Å^2, and for the D_3CF species, it was ~0.35 u Å^2 (where the expected rigid value is 3.23795(1) u Å^2).[21] This nonphysical behavior is taken as evidence of large amplitude motions and will be discussed

TABLE 2: Rotational Transition Frequencies for the Normal Isotopic Species of the Methyl Fluoride−OCS Complex

$J'_{K_aK_c}$	→	$J''_{K_aK_c}$	ν_{obs}/MHz	$\Delta\nu$/MHz[a]
2_{12}		1_{11}	5701.8784	0.0021
1_{10}		1_{01}	5973.8515	−0.0015
2_{02}		1_{01}	5996.4583	0.0002
2_{11}		2_{02}	6292.8750	0.0039
2_{11}		1_{10}	6315.4791	0.0029
3_{12}		3_{03}	6793.7636	0.0029
4_{04}		3_{13}	6942.7631	0.0007
4_{13}		4_{04}	7502.1803	−0.0025
5_{14}		5_{05}	8449.3637	−0.0016
3_{13}		2_{12}	8545.1430	−0.0056
1_{11}		0_{00}	8671.3740	−0.0013
3_{03}		2_{02}	8964.2031	−0.0050
3_{22}		2_{21}	9013.1396	−0.0002
3_{21}		2_{20}	9061.4805	0.0028
3_{12}		2_{11}	9465.1004	0.0027
6_{15}		6_{06}	9667.8951	−0.0004
5_{05}		4_{14}	10345.7312	−0.0057
2_{12}		1_{01}	11368.8951	−0.0038
4_{14}		3_{13}	11379.6476	0.0042
4_{04}		3_{03}	11896.1438	0.0001
4_{23}		3_{22}	12007.5214	−0.0002
4_{32}		3_{31}	12041.2373	−0.0030
4_{31}		3_{30}	12043.0331	0.0005
4_{22}		3_{21}	12127.5014	−0.0012
4_{13}		3_{12}	12604.5706	0.0048
6_{06}		5_{15}	13760.2109	−0.0020
3_{13}		2_{02}	13917.5870	−0.0025
5_{15}		4_{14}	14203.1160	−0.0016
5_{05}		4_{04}	14782.6216	0.0037
5_{14}		4_{13}	15729.8060	0.0056

[a] $\Delta\nu = \nu_{obs} - \nu_{calc}$, where ν_{calc} is calculated from the spectroscopic constants in Table 3.

later. The measured rotational transitions for the normal isotopic species are listed in Table 2; the rotational frequencies for the other four isotopic species are available as Supporting Information. All transition frequencies were fitted to a standard Watson *A*-reduction Hamiltonian[22] using the SPFIT program of Herb Pickett;[23] the resulting spectroscopic parameters are shown in Table 3. It is noteworthy that the $D_3CF-OCS$ species has a significantly different Δ_{JK} distortion constant from that of the H_3CF isotopologues despite the fact that the data set comprised many of the same rotational transitions as the other species. This might be interpreted as an indication of the significant changes in the internal motion dynamics and energetics upon deuteration and may at least partially explain the much poorer structural fits which result upon inclusion of the D_3CF data alongside of the H_3CF data in the structure fitting process (see the Structure section).

The ability to fit the rotational transitions to a standard Watson *A*-reduction Hamiltonian would suggest that the assigned spectrum is probably the *A*-state ($m = 0$) spectrum since *E*-state ($m = \pm 1$) transitions would not be expected to fit so well to such a semirigid Hamiltonian. It should be noted that as a result of the search to identify possible internal rotor doublets and *b*-type transitions, a fairly extensive search region was covered, from 5.5 to 9.7 GHz. A number of transitions requiring both methyl fluoride and OCS, some of which displayed very fast first-order Stark effects, remain unassigned within this region; therefore, it is possible that some of these lines may be the as yet unidentified *E*-state transitions or perhaps belong to torsionally excited states.

To try to identify *E*-state transitions in our search region, an estimate of the barrier was carried out by using the value of the planar moment, P_{cc}. This method has been used previously to estimate the barrier to rotation of a CH_3 top for both molecules[24] and for weakly bound complexes.[3] In any analysis of rotational spectra in which large amplitude motions are present, the experimental rotational constants will include contributions from the rotation of the internal rotor. These constants are related to the high-barrier, rigid rotor rotational constants (labeled A_r, B_r, and C_r) by the following equations (assuming a system with an *ab* plane of symmetry)[25]

$$A_{00} = A_r + W_{00}^{(2)} F \rho_a^2$$
$$B_{00} = B_r + W_{00}^{(2)} F \rho_b^2$$
$$C_{00} = C_r \qquad (1)$$

where the dimensionless perturbation coefficients $W_{00}^{(2)}$ are given by Herschbach,[26] F is the reduced rotational constant of the internal rotor,[26] and the ρ_g terms are direction cosines (λ_g) scaled by the ratio of the moment of inertia of the rotor (I_α) to the moment of inertia of the complex (I_g) ($\rho_g = \lambda_g I_\alpha / I_g$); $g = a$, b, or c. Briefly, the procedure is as follows: the rigid rotational constants (A_r, B_r, and C_r) are obtained from a physically reasonable structure (the ab-initio-optimized structures in this case), and the angles between the internal rotor axis and the principal inertial axes are also calculated from this structure to provide the values of λ_g and hence ρ_g. A series of P_{cc} values can then be generated by using $W_{00}^{(2)}$values from the table in Appendix C of ref 26; a plot of P_{cc} as a function of the associated s value (the reduced barrier) allows the reduced barrier (corresponding to the experimentally observed P_{cc} value) to be identified. The reduced barrier can finally be converted to a V_3 barrier using the expression

$$s = \frac{4V_3}{9F} \qquad (2)$$

Using this approach, the experimental planar moment for the normal isotopic species of −0.21938 u Å^2 (for a structure resembling structure II) is reproduced when a reduced barrier, *s*, of approximately 1.07 is used, corresponding to a V_3 value of 13 cm^{-1}. Repeating this procedure (this time using the angular parameters obtained from structure I) leads to a very similar V_3 barrier of 16 cm^{-1}, while use of the data for the $D_3CF-OCS$ species (where P_{cc} = 0.34595 u Å^2, Table 3) leads to a significantly higher reduced barrier of ∼2.55, although this also translates into a V_3 barrier of 16 cm^{-1}. After careful consideration of the variation of the barrier with respect to the angular parameters (ρ_g) and the rigid rotational constants (A_r, B_r, and C_r), our best estimate of the V_3 barrier in $H_3CF-OCS$ is 14.5(50) cm^{-1} (0.17(6) kJ mol^{-1}). However, since it was necessary to extrapolate far below the lowest tabulated value of $s = 8$, the stated uncertainty in this V_3 value should be viewed cautiously. Using a value of V_3 = 14.5 cm^{-1} in the XIAM program[27] predicts $A-E$ splittings in most rotational transitions on the order of several gigahertz. No assignment of any *E* state lines has yet been made, although a more extensive search for possible candidates will form the basis for future studies on this complex. The magnitude of the estimated V_3 in the present study (0.17(6) kJ mol^{-1}) is just under 50% of the value (0.36 kJ mol^{-1}) determined by similar means for the methyl group in the $H_3CF-TFM$ complex;[3] the existence of multiple C−H···F interactions in the latter complex presumably causes a slight increase in the barrier to rotation.

Dipole Moment. Due to a near-degeneracy between the 2_{02} and 1_{10} energy levels, the standard second-order perturbation

TABLE 3: Spectroscopic Parameters for the Five Isotopologues of the $H_3CF-OCS$ Complex[a]

	$H_3CF-OCS$	$H_3{}^{13}CF-OCS$	$H_3CF-O^{13}CS$	$H_3CF-OC^{34}S$	$D_3CF-OCS$
A/MHz	7322.5753(15)	7322.1689(16)	7279.4636(19)	7253.5315(27)	7166.7556(16)
B/MHz	1655.6314(34)	1614.9628(18)	1651.0414(8)	1618.7493(9)	1513.9106(20)
C/MHz	1348.7426(33)	1321.6426(17)	1344.2144(6)	1321.8642(7)	1252.0266(19)
Δ_J/kHz	5.332(23)	5.020(14)	5.294(11)	5.168(11)	4.353(14)
Δ_{JK}/kHz	−24.74(14)	−23.98(9)	−23.91(15)	−25.61(33)	−2.87(9)
δ_J/kHz	1.264(5)	1.186(8)	1.300(9)	1.240(10)	1.022(8)
δ_K/kHz	12.1(17)	11.7(8)	12.1[b]	12.1[b]	14.0(9)
$\Delta\nu_{rms}$/kHz[c]	3.0	2.3	3.2	3.6	3.4
N[d]	30	26	20	16	27
P_{cc}/u Å^2 [e]	−0.21938(15)	−0.21563(6)	−0.2212(1)	−0.2232(1)	0.34595(8)

[a] Errors given in parentheses are a priori errors reported by the SPFIT program. [b] δ_K is fixed at the value obtained for the normal isotopic species. [c] $\Delta\nu_{rms} = [\sum(\nu_{obs} - \nu_{calc})^2/N]^{1/2}$. [d] *N* is the number of fitted transitions. [e] P_{cc} is the planar moment $= 0.5(I_a + I_b - I_c) = \sum_i m_i c_i^2$.

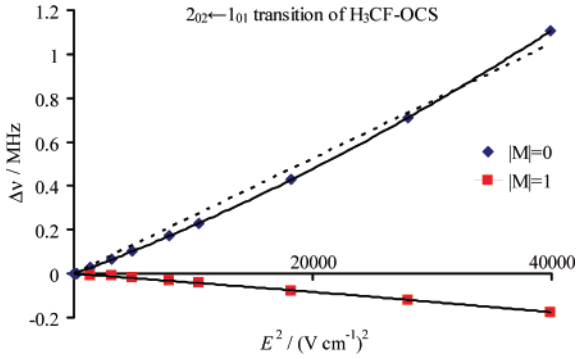

Figure 2. Plot of the Stark effect for the $2_{02} \leftarrow 1_{01}$ transition for the normal isotopic species of the $H_3CF-OCS$ complex. The dashed line superimposed on the data for the $|M| = 0$ component is intended to highlight the deviation from linearity for this component.

theory approach to fitting the dipole moments[28] proved unsatisfactory, with discrepancies between the observed and calculated Stark coefficients of up to 20%. Indeed, clear curvature was observed in some of the $\Delta\nu$ versus E^2 Stark plots for transitions involving these levels (see Figure 2, for example). For this reason, the QSTARK program,[29,30] which allows for diagonalization of the full energy matrix, was utilized to obtain the dipole moment from a fit of 11 $|M|$ components selected from a total of 7 rotational transitions. Applied electric fields up to about 330 V/cm (corresponding to applied voltages of up to ±5 kV) were used. The fast shifts of many transitions at low applied fields reduced the available candidate lines such that some less than optimum transitions (in terms of intensity) had to be included in the data set, leading to a larger than usual uncertainty in the frequency measurements (up to, perhaps, 10 kHz). However, the observed frequency shifts of up to 1 MHz were large compared to the measurement uncertainty, and the resulting dipole moment components were well determined (Table 4), with an overall standard deviation of the fit of 7.3 kHz. A list of the fitted components (61 in all) is included in the Supporting Information. Rotational and centrifugal distortion constants were held fixed at the values obtained from the SPFIT fitting process (Table 3) during the QSTARK fit. Variation of these parameters did not significantly change the standard deviation of the fit or the values of the determined constants. Table 4 also lists the ab initio estimates for structures I and II; agreement with the experimental values is quite reasonable. Attempts to fit a μ_c component of the dipole moment resulted in a zero value to within ±0.001 D, consistent with the expectation of an *ab* plane of symmetry.

The fitted dipole moment components may be compared with those that are obtained from a simple projection of the monomer dipole moments ($\mu(H_3CF) = 1.85$ D[31] and $\mu(OCS) = 0.71521(20)$ D[19]) into the principal axis frame of the dimer (giving $\mu_a = 0.96(5)$ D and $\mu_b = 0.65(6)$ D; the errors reflect the variation

TABLE 4: Dipole Moment Components for the $H_3CF-OCS$ Complex. The "Experimental" Column Shows the Result of Fitting the Experimental Data Using the QSTARK Program,[29,30] while the "Calculated" Column Gives the Values Obtained from the MP2/6-311++G(2d,2p) Calculation (BSSE- and ZPE-Uncorrected) for Structures I and II, Respectively

	experimental	calculated structures I, II
μ_a/D	1.0910(15)	1.147, 0.978
μ_b/D	0.4425(10)	0.507, 0.670
μ_c/D	0[a]	0, 0
μ_{total}/D	1.1773(18)	1.254, 1.186
N[b]	61	–
std. dev./kHz[c]	7.3	–

[a] μ_c was fixed at zero. Attempts to fit this parameter give values that are zero to within the reported uncertainty (to about ±0.001 D). See the text for further discussion. [b] *N* is the number of Stark measurements included in the fit. [c] The standard deviation of the fit.

in the structural parameters that is observed by varying the particular combination of moments of inertia fitted). Even considering the rather large uncertainties attributed to the projected dipole components, it is apparent that only a small enhancement of about 0.1 D for μ_a and a similarly sized reduction in the μ_b component accompanies complex formation.

Structure. Despite the contamination of the moments of inertia by the large amplitude motions, it is still possible to obtain structural information for this complex. With the usual assumption that the monomer structures are held fixed at their literature geometries,[32] a total of three parameters are required to define the structure of this dimer— an intermolecular C···C separation distance ($R_{C\cdots C}$) and two angles to describe the tilt of the symmetry axes of the monomers with respect to the intermolecular distance (θ and ϕ); see Figure 1 for the definition of these structural parameters. Inertial fits were carried out using the STRFITQ program of Schwendeman.[33] A series of fits were carried out using different sets of inertial data to explore the variation in the structural parameters. Because of the unphysical planar moments, it is not possible to obtain good-quality structural fits by including all three moments of inertia for each isotopic species; therefore, all possible combinations (I_a, I_b, and I_c), (I_a, I_b), (I_b, I_c), or (I_a, I_c) were explored to allow an estimation of the optimum structural parameters and their uncertainties. Note that a least-squares fitting of the parameters $R_{C\cdots C}$, θ, and ϕ to the experimental moments of inertia gives identical results for a structure based either on ab initio structure I or II (i.e., the two orientations of the H_3CF cannot be distinguished based on the results of the least-squares fit); therefore, only structure II will be considered for the rest of this discussion. The fitted structural parameters ($R_{C\cdots C}$, θ, ϕ) are given in Table 5. Exclusion of the inertial data for the deuterated (D_3CF) species from the list of isotopic data significantly improves the standard

TABLE 5: Structural Parameters Resulting from Least-Squares Fits of the Moments of Inertia for the Isotopic Species of $H_3CF-OCS$; See the Text for an Explanation of the Different Data Sets Included in This Table

	R/Å	θ/degrees	ϕ/degrees	std. dev./u Å^2
		All Isotopic Data[a]		
I_a, I_b, I_c	3.731(74)	50.9(56)	59.7(22)	1.60
I_a, I_b	3.694(31)	51.7(23)	58.37(92)	0.47
I_a, I_c	3.750(30)	49.5(23)	59.19(93)	0.46
I_b, I_c	3.748(10)	51.64(73)	61.55(30)	0.21
		All H_3CF Data[b]		
I_a, I_b, I_c	3.77(24)	48(18)	61.0(75)	1.44
I_a, I_b	3.771(10)	46.19(79)	60.78(32)	0.044
I_a, I_c	3.779(16)	47.3(13)	60.23(50)	0.065
I_b, I_c	3.7703(55)	49.85(41)	62.12(17)	0.033
best fit[c]	3.75(3)	50(2)	61(2)	

[a] Fitting the $H_3CF-OCS$, $H_3{}^{13}CF-OCS$, $H_3CF-O^{13}CS$, $H_3CF-OC^{34}S$, and $D_3CF-OCS$ moments of inertia. [b] Fitting the same as in footnote a, with the exception that the $D_3CF-OCS$ moment of inertia data is omitted from the fit. [c] The best fit value is an attempt to incorporate all of the values in the above table into a "best-guess" value for each structural parameter.

deviation of the structural fit, and therefore, parameters determined from all of the same combinations of moments but using only the H_3CF data (and omitting the D_3CF data) are also included in the table for comparison. The "best fit value" (presented at the bottom of Table 5) takes into account the variation of all structural parameters from all fits. In a comparison with the ab initio parameters listed in Table 1, it is clear that the two tilt angles lie between the calculated values for the two structures, perhaps closer to structure II, while the C···C distance of 3.75 Å agrees perfectly with either the uncorrected value for structure I or the BSSE+ZPE-corrected value for structure II. Of course, the ab initio values refer to an equilibrium structure, and the distance might therefore be expected to differ by as much as a few hundredths of an angstrom, particularly in a floppy complex with significant internal motion. In any case, it is very likely that, in light of the large amplitude motions, the experimental structure is more of an average of the two structures I and II.

The availability of single isotopic substitution data for certain atoms in the complex ($H_3{}^{13}CF-OCS$, $H_3CF-O^{13}CS$, and $H_3CF-OC^{34}S$) allows for a determination of the Kraitchman coordinates[34] for the substituted atoms. These coordinates were determined for the singly substituted isotopic species using the KRA program of Z. Kisiel.[35] Table 6 lists the derived coordinates, where they are presented alongside of the principal axis coordinates from the uncorrected MP2 calculation and from the inertial fit described above. Given the large amplitude motions, the agreement is quite reasonable, and again, a preference for structure II is evident, with the Kraitchman coordinates agreeing slightly better with the ab initio coordinates for structure II than those for structure I. It is clear that the derived *c*-coordinate of the carbon atom of the H_3CF subunit is nonzero and that the *b*-coordinate for this atom is also not well determined and in poor agreement with the ab initio or inertial fit values. This might be construed as an indication that the internal rotation axis may not coincide with the C_3 axis and maybe that the carbon atom of the methyl fluoride subunit does make some small amplitude excursions from the symmetry plane during the course of the internal motion.

From the derived Kraitchman coordinates, the C═S bond distance is calculated to be 1.564(3) Å, agreeing well with the literature value[32] of 1.5651 Å, while the C···C intermolecular distance is found to be 3.755(6) Å, which (as seen in Tables 1 and 5) is again in excellent agreement with the inertial fit and ab initio values. The C···C−S angle can be calculated to be 61.8(5)°, in near-perfect agreement with the inertial fit value of 61(2)° (Table 5). Despite contamination of the moments of inertia by the internal motion, the resulting structural parameters seem very reasonable, and we feel that they reflect accurately the true structure of this complex.

TABLE 6: Principal Axis Coordinates[a] Derived from the Kraitchman Single Substitution Calculations, Inertial Fit, and Ab Initio Optimizations (in Angstroms). Note That Only the Coordinate's Magnitude, and Not the Sign, Is Determined from Kraitchman's Equations

	principal axis coordinates[b]/Å		
	a	*b*	*c*
$H_3{}^{13}CF$	2.7819(6)	0.010(160)	0.062(25)
	2.762(20)	0.087(16)	0.000
	2.7018; 2.7825	0.09878; 0.05851	0.000; 0.000
$O^{13}CS$	0.9238(17)	0.6448(24)	0.050*i*(31)
	−0.928(17)	0.645(5)	0.000
	−0.8867; −0.9221	0.6375; 0.6445	0.000; 0.000
$OC^{34}S$	1.8843(8)	0.5899(26)	0.044*i*(34)
	−1.903(18)	−0.579(23)	0.000
	−1.9151; −1.8968	−0.5451; −0.5824	0.000; 0.000

[a] The listed uncertainties in the Kraitchman coordinates reflect the sum of propagated uncertainties from the rotational constants and the Costain error. [b] Each principal axis coordinate has been derived from three sources; the Kraitchman single substitution coordinate ("R_s") is given on the first line, followed by the inertial fit value ("R_0"), and the third line lists the two uncorrected ab initio values (from structures I and II, respectively). The inertial fit value uncertainty encompasses the full range of coordinates obtained from fitting the different sets of moments (see Table 5).

Discussion

Comparison of the $R_{C\cdots C}$ distances derived in this complex with those listed in Table 7 for TFM−OCS reveals this distance to be about 0.11 Å longer for $H_3CF-OCS$ than that for the TFM−OCS complex, while the center of mass separation for $H_3CF-OCS$ is considerably shorter than that in TFM−OCS (by ∼0.37 Å). The O···H distance resulting from the inertial fits for $H_3CF-OCS$ is determined to be 2.65(6) Å, some 0.25 Å shorter than the O···H distance seen in the TFM−OCS complex (2.90(5) Å),[12] although still longer than that observed in some of the multiply bonded complexes of TFM such as dioxane−TFM (2.315(85) Å),[4] cyclobutanone−TFM (2.40(1) Å),[6] and oxirane−TFM (2.42(2) Å).[1]

A comparison of the binding energies (E_B) estimated using the relationship[36] $E_B = (1/72)k_s R_{CM}^2$ (with the force constant for the weak bond (k_s) coming from use of the pseudodiatomic approximation[12,37]) indicates that the binding energy in $H_3CF-OCS$ (3.5(1) kJ mol^{-1}) is more than twice that for the TFM−OCS complex (1.6(1) kJ mol^{-1}),[12] perhaps as a result of the increased electrostatic interaction arising from the slightly more polar H_3CF (μ = 1.85 D)[31] compared to the TFM (μ = 1.65 D).[31] Interestingly, the binding energy for the methane complex with OCS is found to be very close to that for the MeF−OCS complex, despite the nonpolar nature of the CH_4 subunit. The $R_{C\cdots C}$ and R_{CM} separations of the CH_4-OCS complex[38] fall between the values of the TFM and H_3CF species, although the angle O−C···C is considerably larger. Of course, these binding energy calculations are subject to several assumptions, and the highly dynamic nature of the CH_4-OCS complex also introduces additional uncertainty into the binding energy calculation; therefore, any apparent trends should be viewed with caution. Additionally, the CH_4-OCS complex is unique in this data set since the methane portion is nonpolar and a

TABLE 7: Structural Parameters for the Fluorinated Methane Complexes HCF_3−OCS and H_3CF−OCS. Data for the CH_4−OCS Complex Have Also Been Included for Comparison

complex	$R_{C\cdots C}$/Å	R_{CM}/Å	angle O−C···C/°	E_B/kJ mol^{-1}	reference
HCF_3−OCS	3.642(17)	3.965(26)	60.2(4)	1.6(1)	12
H_3CF−OCS	3.75(3)	3.60(3)	61(2)	3.5(1)	this work
CH_4−OCS	3.68 [3.74][a]	3.81 [3.85]	80 [82][a]	3.4(1)	38

[a] The CH_4 subunit in the CH_4−OCS complex exhibited tumbling motions, and therefore, the first value refers to a distance or angle derived in the rigid rotor limit and the second value [given in brackets] in the free rotor limit for the CH_4 rotation.

tumbling motion of the CH_4 unit gives rise to the appearance of *A* and *T* librational states in the rotational spectrum.

Finally, the binding energy in the present case of H_3CF−OCS is found to be about two-thirds that of the value in the H_3CF−TFM complex (5.3 kJ mol^{-1}),[3] as a result of the multiple C−H···F interactions in the latter complex leading to an increased strength of binding.

Conclusions

The rotational spectra for five isotopic species of the weakly bound complex between H_3CF and OCS have been measured. The closeness in energy of the two lowest-energy structures I and II (Figure 1) obtained from ab initio calculations makes it impossible to favor one or the other as the minimum-energy configuration, and in light of the expected small barrier to interconversion, it seems likely that significant internal rotation of the methyl top occurs. No *E* state lines or torsionally excited states have yet been identified in the rotational spectrum, but attempts to assign these spectra are underway, utilizing a barrier estimate of 14.5(50) cm^{-1}, which has been obtained from the P_{cc} planar moment. Structural parameters from inertial fits and single isotopic substitution calculations are in reasonable agreement with ab initio values, and, again, given the rather large uncertainties in the fitted structural parameters arising from the large amplitude motion and the closeness of the predicted ab initio values, it is difficult to express a preference for I or II.

In this dimer, and in other weakly bound complexes studied at similar levels of calculations, inclusion of BSSE and ZPE corrections can sometimes diminish the quality of agreement with the experimental structural parameters relative to results computed with no such corrections. When different conformers are separated by a small energy barrier, it is difficult to obtain quantitative predictions of these barriers, and even the relative stabilities may be subject to variation at differing levels of calculation. The results of the ab initio calculations in the present study therefore serve to highlight the need for more experimental data to act as a benchmark for improving such calculations.

Acknowledgment. The authors acknowledge the donors of the ACS Petroleum Research Fund (PRF 39752-GB6) for partial support of this work. The authors also thank Dr. Rebecca Peebles for helpful input during the preparation of the manuscript.

Supporting Information Available: Tables of measured transition frequencies and residuals from the least-squares fitting process for the four isotopically substituted species and the results from the least-squares fit of the dipole moment using the QSTARK program. This material is available free of charge via the Internet at http://pubs.acs.org.

References and Notes

(1) Alonso, J. L.; Antolínez, S.; Blanco, S.; Lesarri, A.; López, J. C.; Caminati, W. *J. Am. Chem. Soc.* **2004**, *126*, 3244.

(2) Cocinero, E. J.; Sanchez, R.; Blanco, S.; Lesarri, A.; López, J. C.; Alonso, J. L. *Chem. Phys. Lett.* **2005**, *402*, 4.

(3) Caminati, W.; López, W. C.; Alonso, J. L.; Grabow, J.-U. *Angew. Chem., Int. Ed*. **2005**, *44*, 3840.

(4) Favero, L. B.; Giuliano, B. M.; Melandri, S.; Maris, A.; Ottaviani, P.; Velino, B.; Caminati, W. *J. Phys. Chem. A* **2005**, *109*, 7402.

(5) López, J. C.; Caminati, W.; Alonso, J. L. *Angew. Chem., Int. Ed.* **2005**, *45*, 290.

(6) Ottaviani, P.; Caminati, W.; Favero, L. B.; Blanco, S.; López, J. C.; Alonso, J. L. *Chem.—Eur. J.* **2006**, *12*, 915.

(7) Blanco, S.; López, J. C.; Lesarri, A.; Caminati, W.; Alonso, J. L. *ChemPhysChem* **2004**, *5*, 1779.

(8) Blanco, S.; López, J. C.; Lesarri, A.; Alonso, J. L. *J. Mol. Struct.* **2002**, *612*, 255.

(9) Caminati, W.; Melandri, S.; Moreschini, P.; Favero, P. G. *Angew. Chem., Int. Ed.* **1999**, *38*, 2924.

(10) Caminati, W.; Melandri, S.; Schnell, M.; Banser, D.; Grabow, J.-U.; Alonso, J. L. *J. Mol. Struct.* **2005**, *742*, 87.

(11) Blanco, S.; Melandri, S.; Ottaviani, P.; Caminati, W. *J. Am. Chem. Soc.* **2007**, *129*, 2700.

(12) Serafin, M. M.; Peebles, S. A. *J. Phys. Chem. A* **2006**, *110*, 11938.

(13) Serafin, M. M.; Peebles, S. A. **2007**, manuscript in preparation.

(14) Serafin, M. M.; Peebles, R. A.; Peebles, S. A. **2007**, manuscript in preparation.

(15) Peebles, S. A.; Serafin, M. M.; Peebles, R. A. 61st International Symposium on Molecular Spectroscopy, Talk MH13; Columbus, OH, 2006.

(16) Balle, T. J.; Flygare, W. H. *Rev. Sci. Instrum.* **1981**, *52*, 33.

(17) Newby, J. J.; Serafin, M. M.; Peebles, R. A.; Peebles, S. A. *Phys. Chem. Chem. Phys*. **2005**, *7*, 487.

(18) Grabow, J.-U. Ph.D. Thesis, University of Kiel, Kiel, Germany, 1992.

(19) Muenter, J. S. *J. Chem. Phys.* **1968**, *48*, 4544.

(20) Frisch, M. J.; Trucks, G. W.; Schlegel, H. B.; Scuseria, G. E.; Robb, M. A.; Cheeseman, J. R.; Montgomery, J. A., Jr.; Vreven, T.; Kudin, K. N.; Burant, J. C.; Millam, J. M.; Iyengar, S. S.; Tomasi, J.; Barone, V.; Mennucci, B.; Cossi, M.; Scalmani, G.; Rega, N.; Petersson, G. A.; Nakatsuji, H.; Hada, M.; Ehara, M.; Toyota, K.; Fukuda, R.; Hasegawa, J.; Ishida, M.; Nakajima, T.; Honda, Y.; Kitao, O.; Nakai, H.; Klene, M.; Li, X.; Knox, J. E.; Hratchian, H. P.; Cross, J. B.; Bakken, V.; Adamo, C.; Jaramillo, J.; Gomperts, R.; Stratmann, R. E.; Yazyev, O.; Austin, A. J.; Cammi, R.; Pomelli, C.; Ochterski, J. W.; Ayala, P. Y.; Morokuma, K.; Voth, G. A.; Salvador, P.; Dannenberg, J. J.; Zakrzewski, V. G.; Dapprich, S.; Daniels, A. D.; Strain, M. C.; Farkas, O.; Malick, D. K.; Rabuck, A. D.; Raghavachari, K.; Foresman, J. B.; Ortiz, J. V.; Cui, Q.; Baboul, A. G.; Clifford, S.; Cioslowski, J.; Stefanov, B. B.; Liu, G.; Liashenko, A.; Piskorz, P.; Komaromi, I.; Martin, R. L.; Fox, D. J.; Keith, T.; Al-Laham, M. A.; Peng, C. Y.; Nanayakkara, A.; Challacombe, M.; Gill, P. M. W.; Johnson, B.; Chen, W.; Wong, M. W.; Gonzalez, C.; Pople, J. A. *Gaussian 03*, revision D.01; Gaussian, Inc.: Wallingford, CT, 2004.

(21) Demaison, J.; Breidung, J.; Thiel, W.; Papousek, D. *Struct. Chem.* **1999**, *10*, 129.

(22) Watson, J. K. G. *Vib. Spectra Struct.* **1977**, *6*, 1.

(23) Pickett, H. M. *J. Mol. Spectrosc.* **1991**, *148*, 371.

(24) Caminati, W.; Di Bernardo, S. *Chem. Phys. Lett.* **1990**, *17*, 39.

(25) Herschbach, D. R.; Swalen, J. D. *J. Chem. Phys.* **1958**, *29*, 761.

(26) Herschbach, D. R. *J. Chem. Phys*. **1959**, *31*, 91.

(27) Hartwig, H.; Dreizler, H. *Z. Naturforsch., A: Phys. Sci*. **1996**, *51*, 923.

(28) Second-order Stark coefficients were calculated using a modified version of the original ASYSPEC code; see Beaudet, R. A., Ph.D. Thesis, Harvard University, Cambridge, MA, 1961.

(29) Kisiel, Z.; Kosarzewski, J.; Pietrewicz, B. A.; Pszczółkowski, L. *Chem. Phys. Lett.* **2000**, *325*, 523.

(30) Kisiel, Z. PROSPE—Programs for Rotational Spectroscopy. http://info.ifpan.edu.pl/~kisiel/prospe.htm (accessed Aug 2007).

(31) Nelson, R. D.; Lide, D. R.; Maryott, A. A. In *Selected Values of Electric Dipole Moments for Molecules in the Gas Phase*; NIST Standard Reference Database, NBS10: Washington, DC, 1967.

(32) Harmony, M. D.; Laurie, V. W.; Kuczkowski, R. L.; Schwendeman, R. H.; Ramsay, D. A.; Lovas, F. J.; Lafferty, W. J.; Maki, A. J. *J. Phys. Chem. Ref. Data* **1979**, *8*, 619.

(33) Schwendeman, R. H. In *Critical Evaluation of Chemical and Physical Structural Information*; Lide, D. R., Paul, M. A., Eds.; National Academy of Sciences: Washington, DC, 1974. The STRFITQ program used in this work is the University of Michigan modified version of Schwendeman's original code.

(34) Kraitchman, J. *Am. J. Phys.* **1953**, *21*, 17.

(35) Kraitchman coordinates and propagated errors were calculated using the KRA code; see Kisiel, Z. PROSPE—Programs for Rotational Spectroscopy. http://info.ifpan.edu.pl/~kisiel/prospe.htm (accessed June 2007).

(36) Read, W. G.; Campbell, E. J.; Henderson, G. *J. Chem. Phys.* **1983**, *78*, 3501.

(37) Millen, D. J. *Can. J. Chem.* **1985**, *63*, 1477.

(38) Hearn, J. P. I.; Howard, B. J. *Mol. Phys.* **2002**, *100*, 2679.